

# Mechanistic Investigations of the ZnCl<sub>2</sub>-Mediated Tandem Mukaiyama Aldol Lactonization: Evidence for Asynchronous, Concerted Transition States and Discovery of 2-Oxopyridyl Ketene Acetal Variants

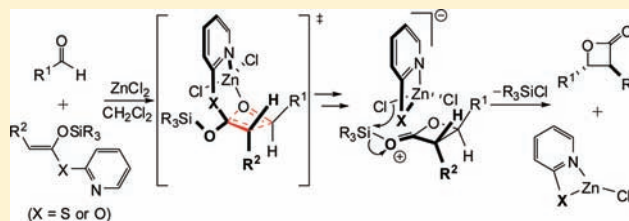
Cunxiang Zhao,<sup>†,⊥</sup> T. Andrew Mitchell,<sup>\*,†,‡</sup> Ravikrishna Vallakati,<sup>†</sup> Lisa M. Pérez,<sup>\*,#</sup> and Daniel Romo<sup>\*,†</sup>

<sup>†</sup>Department of Chemistry and <sup>#</sup>Laboratory for Molecular Simulation, Texas A&M University, P.O. Box 30012, College Station, Texas 77842-3012, United States

<sup>‡</sup>Department of Chemistry, Illinois State University, Campus Box 4160, Normal, Illinois 61790-4160, United States

**S** Supporting Information

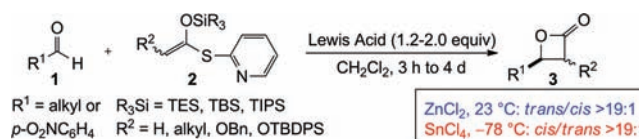
**ABSTRACT:** The ZnCl<sub>2</sub>-mediated tandem Mukaiyama aldol lactonization (TMAL) reaction of aldehydes and thiopyridyl ketene acetals provides a versatile, highly diastereoselective approach to *trans*-1,2-disubstituted  $\beta$ -lactones. Mechanistic and theoretical studies described herein demonstrate that both the efficiency of this process and the high diastereoselectivity are highly dependent upon the type of ketene acetal employed but independent of ketene acetal geometry. Significantly, we propose a novel and distinct mechanistic pathway for the ZnCl<sub>2</sub>-mediated TMAL process versus other Mukaiyama aldol reactions based on our experimental evidence to date and further supported by calculations (B3LYP/BSI). Contrary to the commonly invoked mechanistic extremes of [2+2] cycloaddition and aldol lactonization mechanisms, investigations of the TMAL process suggest a concerted but asynchronous transition state between aldehydes and thiopyridyl ketene acetals. These calculations support a boat-like transition state that differs from commonly invoked Mukaiyama “open” or Zimmerman–Traxler “chair-like” transition-state models. Furthermore, experimental studies support the beneficial effect of pre-coordination between ZnCl<sub>2</sub> and thiopyridyl ketene acetals prior to aldehyde addition for optimal reaction rates. Our previously proposed, silylated  $\beta$ -lactone intermediate that led to successful TMAL-based cascade sequences is also supported by the described calculations and ancillary experiments. These findings suggested that a similar TMAL process leading to  $\beta$ -lactones would be possible with an oxopyridyl ketene acetal, and this was confirmed experimentally, leading to a novel TMAL process that proceeds with efficiency comparable to that of the thiopyridyl system.



## INTRODUCTION

Due to the versatility of the  $\beta$ -lactone (2-oxetanone) nucleus, several groups have recently pursued the development of stereoselective routes to these strained heterocycles and their application to natural product synthesis.<sup>1</sup> Two of the most widely employed strategies to construct these heterocycles directly from aldehydes are [2+2] cycloadditions with ketenes or ketene equivalents<sup>2</sup> and tandem aldol lactonizations with enolates or enolate equivalents.<sup>3</sup> Although Staudinger first introduced the synthesis of  $\beta$ -lactones via the [2+2] cycloaddition in 1911,<sup>4</sup> it was not until 1982 that Wynberg achieved an effective asymmetric synthesis of  $\beta$ -lactones proceeding through a proposed aldol-lactonization process.<sup>5</sup> Utilizing ketenes and catalytic amounts of *Cinchona* alkaloids, presumed ammonium enolates were generated and provided  $\beta$ -lactones when reacted with highly electrophilic aldehydes, such as chloral. Since this groundbreaking achievement, stereoselective routes to  $\beta$ -lactones have increased dramatically.<sup>1</sup> Building on a single example described by Hirai,<sup>6</sup> we have extensively developed the tandem Mukaiyama aldol lactonization (TMAL) reaction of aldehydes **1** and thiopyridyl ketene acetals **2** with both SnCl<sub>4</sub><sup>7</sup> and ZnCl<sub>2</sub><sup>8</sup> for the diastereoselective synthesis of either *cis*- or *trans*- $\beta$ -lactones **3**, respectively (Scheme 1). We<sup>9</sup>

### Scheme 1. Synthesis of *cis*- and *trans*- $\beta$ -Lactones Promoted by SnCl<sub>4</sub> and ZnCl<sub>2</sub>



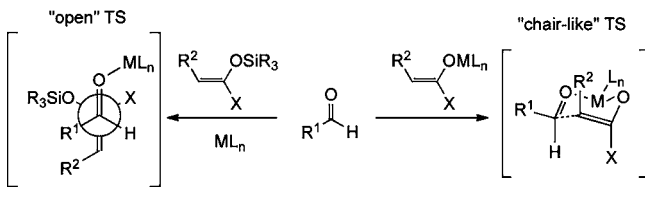
and others<sup>10</sup> have utilized the TMAL process to access both racemic and optically active  $\beta$ -lactones with high diastereoselectivity. For example, the TMAL process was utilized in the total synthesis of (–)-panclicin D,<sup>8</sup> tetrahydrolipstatin/orlistat and derivatives,<sup>11</sup> okinonellin B,<sup>12</sup> brefeldin A,<sup>13</sup> and belactosin C.<sup>14</sup> The TMAL reaction was also recently employed to access activity-based probes premised on the tetrahydrolipstatin core to determine off-targets of this potential anticancer agent<sup>15</sup> which is known to inhibit the thioesterase domain of mammalian fatty acid synthase.<sup>16</sup>

Received: September 29, 2011

Published: December 30, 2011

The Mukaiyama aldol reaction<sup>17</sup> is a venerable, benchmark reaction for the formation of C–C bonds and typically proceeds through an open transition state in contrast to the cyclic Zimmerman–Traxler transition states typical of aldol reactions involving metalated enolates (Scheme 2).<sup>18</sup> In contrast, we now

**Scheme 2. Commonly Invoked Transition-State Arrangements for Mukaiyama Aldol Reactions (Open Transition State, TS) and Metalated Enolate Aldols (Zimmerman–Traxler, Chairlike TS)**



describe detailed experimental and computational studies that support a unique transition-state arrangement for the  $\text{ZnCl}_2$ -mediated tandem Mukaiyama aldol-lactonization process that directly delivers  $\beta$ -lactones. In particular, a novel asynchronous, concerted pathway for the  $\text{ZnCl}_2$ -mediated TMAL process proceeding through transition state (*E*)-4 involving tetrahedral zinc(II) and a functional, silylated  $\beta$ -lactone (*E*)-5 intermediate are supported by B3LYP/BSI calculations<sup>19</sup> of the TMAL process (Figure 1a). Several features of the TMAL reaction that

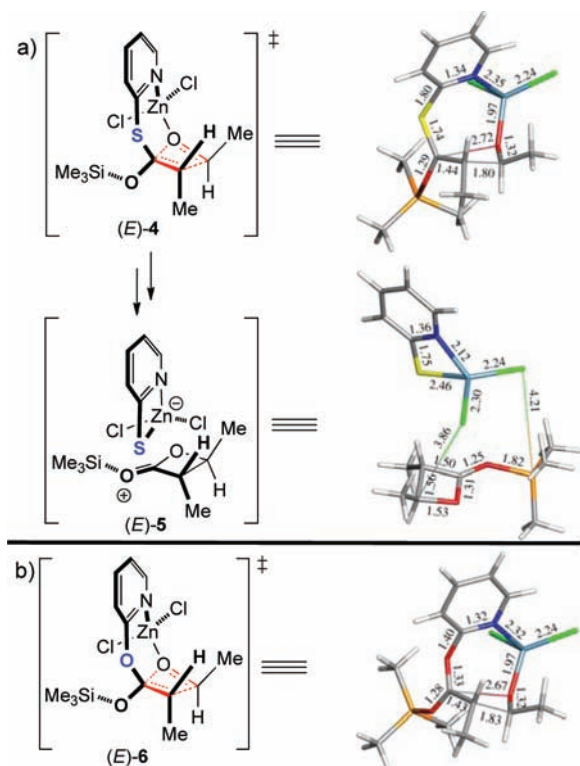


**Figure 1.** Unique features of the  $\text{ZnCl}_2$ -mediated TMAL process. B3LYP/BSI optimized structures showing asynchronous concerted transition states for (a) thiopyridyl ketene acetal (*E*)-4 and (b) a new oxopyridyl ketene acetal (*E*)-6 and a versatile, silylated  $\beta$ -lactone intermediate (*E*)-5 with a thiopyridyl dichlorozincate counterion.

were uncovered in the course of these studies<sup>20</sup> include: (1) lack of dependence on  $\alpha$ -substitution (i.e., *gem*-dialkyl or vic-

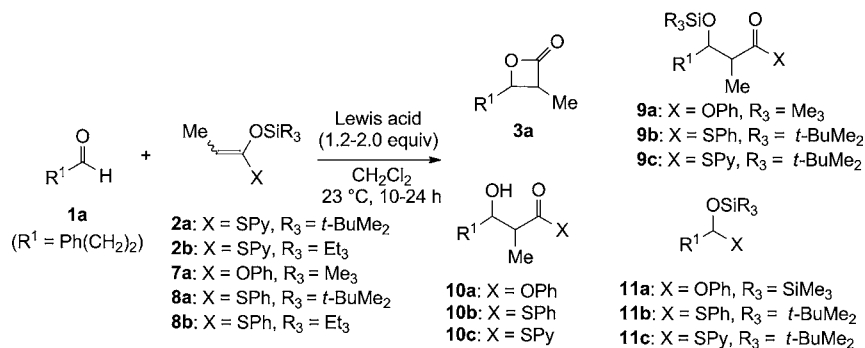
dialkyl effects<sup>21</sup>) was observed unlike related lactonization processes that deliver  $\beta$ -lactones,<sup>22</sup> (2) only stoichiometric quantities of  $\text{ZnCl}_2$  and  $\text{SnCl}_4$  efficiently promote the reaction and no detectable quantities of typical aldol products (i.e.,  $\beta$ -hydroxy and/or  $\beta$ -silyloxy thiopyridyl esters) were observed with these Lewis acids, (3) aliphatic aldehydes and *p*-nitrobenzaldehyde were reactive, but ketones were unreactive, (4) with respect to ketene acetal geometry, stereoconvergence was observed with aliphatic, achiral aldehydes leading to observed high diastereoselectivity for *trans*- $\beta$ -lactones with the exception of *p*-nitrobenzaldehyde (*vide infra*). The described studies led to optimization of the TMAL process through the identification of the silylated  $\beta$ -lactone intermediate (*E*)-5 that could also be intercepted to access novel tandem or cascade processes including a route to  $\beta$ -chlorosilyl esters<sup>7</sup> and a cascade, three-component synthesis of tetrahydrofurans (THFs)<sup>23</sup> and tetrahydropyrans (THPs).<sup>24</sup> Finally, we describe a new TMAL reaction employing an oxopyridyl ketene acetal, which was predicted to react in a similar manner based on B3LYP/BSI calculations (see Figure 1b). This was indeed verified experimentally to deliver *trans*- $\beta$ -lactones in comparable yields to sulfur analogues.

## RESULTS AND DISCUSSION

**Optimization of the TMAL Process: The Indispensable Pyridyl Moiety<sup>25</sup> for Efficient  $\beta$ -Lactone Formation and High Diastereoselectivity.** During early optimization studies of the TMAL process with hydrocinnamaldehyde (**1a**) and ketene acetals **2**, **7**, and **8**, we discovered that the formation of  $\beta$ -lactones, as opposed to typical aldol adducts, was highly dependent on the ketene acetal and Lewis acid employed in terms of both product distribution and diastereoselectivity (Table 1). Use of phenoxy ketene acetal **7a** (*E/Z*, 7:1) with  $\text{BF}_3 \cdot \text{OEt}_2$ ,  $\text{TiCl}_4$ , and  $\text{MgCl}_2$  delivered primarily aldol adduct **10a** (entries 1, 2) or led to no reaction (entry 3).<sup>26</sup> Application of  $\text{MgBr}_2 \cdot \text{OEt}_2$  at reduced temperature ( $-40^\circ\text{C}$ ) to avoid known reactions of  $\beta$ -lactones with this Lewis acid (e.g., dyotropic rearrangements<sup>27</sup>), delivered  $\beta$ -lactone **3a** in 23% yield and excellent diastereoselectivity (>19:1) favoring the *trans*- $\beta$ -lactone, but accompanied by significant quantities of aldol adducts **9a/10a** (entry 4).  $\text{ZnCl}_2$  also delivered appreciable yields (20%) of  $\beta$ -lactone **3a**, but with poor diastereoselectivity (~2:1) along with greater quantities of aldol adduct **9a** (entry 5).

When the *tert*-butyldimethylsilyl (TBS) thiophenyl ketene acetal **8a** (*E/Z*, 20:1) was utilized with  $\text{ZnCl}_2$ ,  $\beta$ -lactone **3a** was isolated in 16% yield along with significant quantities of aldol adducts **9b** (40%) and thioacetal byproduct **11b** (17%, entry 6).  $\beta$ -Lactone **3a** was not isolated when triethylsilyl (TES) thiophenyl ketene acetal **8b** (*E/Z*, 1:7) was employed with  $\text{TiCl}_4$ , rather only aldol adduct **10c** was isolated in 57% yield (entry 7). Although the yield of  $\beta$ -lactone **3a** increased (32–35%) when TES (*E*- or (*Z*)-thiophenyl ketene acetals **8b** were employed with  $\text{ZnCl}_2$ , diastereoselectivity was poor (~2:1), and this reaction led to comparable combined yields of  $\beta$ -silyloxy thiophenyl ester **9c** and thioacetal **11c** (35–42%) (entries 8, 9). As previously described,<sup>8,9</sup> the use of TES thiopyridyl ketene acetals **2b** led to optimal yields of  $\beta$ -lactone **3a** (70%) as a single diastereomer (dr, >19:1) with no aldol adducts detected by  $^1\text{H}$  NMR analysis of the crude reaction mixture and only trace quantities of thioacetal **11d** (entry 10).<sup>8a</sup> In contrast, reduced yields but high diastereoselectivity were obtained with TBS thiopyridyl ketene acetals **2a** (*E/Z*, 20:1,

Table 1. Dependence of the TMAL Process on Ketene Acetal and Lewis Acid: Product Distribution and Diastereoselectivity



entry	X	SiR <sub>3</sub>	E:Z ratio	Lewis acid	3a <sup>a</sup> % yield	3a <sup>b</sup> dr	9a-c <sup>a</sup> % yield	10a-c <sup>a</sup> % yield	11a-c <sup>a</sup> % yield
1	OPh	TMS	7:1	BF <sub>3</sub> ·OEt <sub>2</sub> <sup>d</sup>	<5 <sup>c</sup>	NA <sup>g</sup>	<5 <sup>c</sup>	62	<5 <sup>c</sup>
2	OPh	TMS	7:1	TiCl <sub>4</sub> <sup>e</sup>	<5 <sup>c</sup>	NA <sup>g</sup>	<5 <sup>c</sup>	61	<5 <sup>c</sup>
3	OPh	TMS	7:1	MgCl <sub>2</sub>	<5 <sup>c</sup>	NA <sup>g</sup>	<5 <sup>c</sup>	<5 <sup>c</sup>	<5 <sup>c</sup>
4	OPh	TMS	7:1	MgBr <sub>2</sub> ·OEt <sub>2</sub> <sup>f</sup>	23	>19:1	9	18	<5 <sup>c</sup>
5	OPh	TMS	7:1	ZnCl <sub>2</sub>	20	2.2:1	28	<5 <sup>c</sup>	<5 <sup>c</sup>
6	SPh	TBS	20:1	ZnCl <sub>2</sub>	16	1:1	40	<5 <sup>c</sup>	17
7	SPh	TES	1:7	TiCl <sub>4</sub> <sup>e</sup>	<5 <sup>c</sup>	NA <sup>g</sup>	<5 <sup>c</sup>	57	<5
8	SPh	TES	9:1	ZnCl <sub>2</sub>	35	1:1.7	14	<5 <sup>c</sup>	21
9	SPh	TES	1:7	ZnCl <sub>2</sub>	32	2.0:1	16	<5 <sup>c</sup>	26
10	SPy	TES	7:1	ZnCl <sub>2</sub>	70	>19:1	<5 <sup>c</sup>	<5 <sup>c</sup>	<5 <sup>c</sup>
11	SPy	TES	1:4	ZnCl <sub>2</sub>	70	>19:1	<5 <sup>c</sup>	<5 <sup>c</sup>	<5 <sup>c</sup>
12	SPy	TBS	20:1	ZnCl <sub>2</sub>	57	>19:1	<5 <sup>c</sup>	<5 <sup>c</sup>	<5 <sup>c</sup>

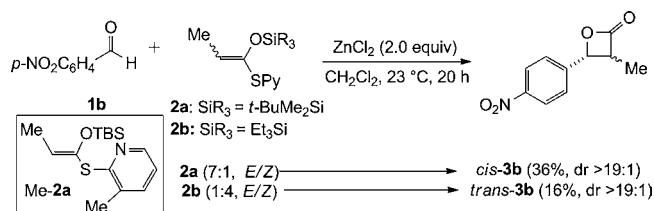
<sup>a</sup>Isolated yield after column chromatography unless otherwise noted. <sup>b</sup>Estimated by <sup>1</sup>H NMR (200 MHz) analysis of the crude reaction mixture. <sup>c</sup>Not detected by <sup>1</sup>H NMR (200 MHz) analysis of the crude reaction mixture. <sup>d</sup>Reaction performed at 0 °C. <sup>e</sup>Reaction performed at -78→0 °C. <sup>f</sup>Reaction performed at -40 °C. <sup>g</sup>Not applicable. <sup>h</sup>See ref 7. TMS = trimethylsilyl; TES = triethylsilyl; TBS = *tert*-butyldimethylsilyl.

entry 12, *vide infra*).<sup>8b,28</sup> Other nitrogen heterocycles (i.e., 3-methylimidazole and 3-methylpyrimidine vs 2-thiopyridyl) were also studied and led to inferior yields of  $\beta$ -lactones.<sup>8b</sup> Taken together, these results point to the critical importance of the combination of a 2-thiopyridyl ketene acetal and ZnCl<sub>2</sub> as Lewis acid<sup>29</sup> for optimal yields of *trans*- $\beta$ -lactones via the TMAL process.

The TMAL process is stereoconvergent with respect to ketene acetal geometry with all aliphatic aldehyde substrates studied to date but not with *p*-nitrobenzaldehyde. Other aromatic aldehydes (e.g., benzaldehyde) lead to  $\beta$ -lactones with benzylic C–O bonds that are labile under TMAL conditions. In Hirai's single reported example of this process leading to  $\beta$ -lactone **3b**, only the *cis*-diastereomer was isolated (23%) in reaction of (*E*)-propionyl ketene acetal Me-**2a** with *p*-nitrobenzaldehyde.<sup>6</sup> We reproduced this result with the non-methylated thiopyridyl ketene acetal (*E*)-**2b** (7:1, *E*/*Z* ratio) with slightly improved yield (36%) to give high diastereoselectivity for the *cis*- $\beta$ -lactone **3b** and the relative stereochemistry was confirmed by X-ray analysis.<sup>8</sup> In contrast, use of (*Z*)-2-thiopyridyl propionyl ketene acetal (4:1, *Z*/*E* ratio) with *p*-nitrobenzaldehyde gave exclusively *trans*- $\beta$ -lactone **3b** (dr >19:1), albeit in only 16% yield (Scheme 3).<sup>30</sup> The low yields observed in these reactions make it difficult to draw definitive conclusions from these results and ascertain the exact nature of the observed, apparent stereospecificity; however, the observed stereodivergence with respect to ketene acetal geometry with *p*-nitrobenzaldehyde is in stark contrast to aliphatic aldehydes but is consistent with our proposed transition states for the TMAL process (*vide infra*).

An additional experiment further demonstrated the superiority of the thiopyridyl moiety compared to the thiophenyl

### Scheme 3. Stereodivergent TMAL Process with *p*-Nitrobenzaldehyde (**1b**) and (*E*)/(*Z*)-Ketene Acetals **2b**

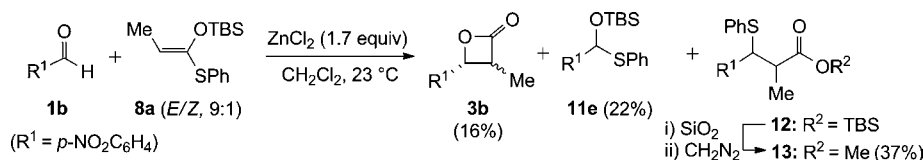


moiety (Scheme 4). When *p*-nitrobenzaldehyde **1b** was treated with thiophenyl ketene acetal (*E*)-**8a** under typical TMAL conditions, the expected  $\beta$ -lactone **3b** was isolated in 16% yield. However, additional byproducts included thioacetal **11e** (22% yield) and a silyl ester byproduct **12** obtained as a mixture of diastereomers. Desilylation occurred during flash column chromatography and the resulting carboxylic acid was treated with diazomethane to aid purification delivering the  $\beta$ -thiophenyl methyl ester **13** in 37% yield over two steps. Related byproducts have never been observed with thiopyridyl ketene acetals, suggesting a reduced nucleophilicity or availability of the thiopyridyl group in comparison to the thiophenyl group, which is likely due to enhanced stability of the bidentate 2-thiopyridine·ZnCl<sub>2</sub> complex compared to a monodentate thiophenyl group.

**Evidence for a Six-Membered, Zinc(II)–Ketene Acetal Complex in the TMAL Reaction.** The stereoconvergent diastereoselectivity and optimal yields of  $\beta$ -lactone **3a** when thiopyridyl ketene acetal **2b** was utilized (cf. Table 1, entries 10, 11) indicates that the nitrogen of the thiopyridyl ring must perform a pivotal function in the TMAL process. One rationale is an



## Scheme 4. TMAL Byproducts with Thiophenyl Ketene Acetal 8a



inductive effect of the nitrogen, but this appears insufficient to explain the sharp difference in diastereoselectivity between these ketene acetals (i.e., thiophenyl **8a** versus thiopyridyl **2a**) and does not correlate with the previously described lack of reactivity when more electron-withdrawing heterocycles were utilized in place of thiopyridyl.<sup>8b</sup> Another explanation invokes Zn(II)–nitrogen coordination leading to a high degree of rigidity in proposed transition-state arrangements. A related cyclic transition state was proposed by Choo and Suh for Ti(IV)-mediated Mukaiyama aldol reactions with thiopyridyl silylketene acetals.<sup>31</sup> In this case, bidentate Lewis acid coordination was invoked between Ti(IV) and both the pyridine nitrogen and a silylether oxygen leading to exclusive formation of the *syn*-aldols independent of the geometry of the ketene acetal (stereoconvergent). However, in the present reaction employing ZnCl<sub>2</sub>, which is also capable of bidentate chelation, the *trans*- $\beta$ -lactone derived from an *anti*-aldol process is the major product obtained for all aliphatic aldehydes studied.

While four-membered Zn–S complexes were invoked in our originally proposed transition-state arrangements<sup>23a</sup> and supported by X-ray crystal structures of related Zn complexes,<sup>32</sup> we were interested in analyzing the structure of the initial ketene acetal·ZnCl<sub>2</sub> complexes, both experimentally and computationally,<sup>19</sup> prior to addition of aldehyde. The <sup>1</sup>H NMR (500 MHz, CDCl<sub>3</sub>) chemical shifts of both uncomplexed and ZnCl<sub>2</sub>-complexed thiopyridyl ketene acetals, (*E*)-**2a** and (*E*)-**2a**·ZnCl<sub>2</sub> (1.0 equiv of **2a**, 1.0 equiv of ZnCl<sub>2</sub>, homogeneous solution in CH<sub>2</sub>Cl<sub>2</sub>), respectively, were determined in CDCl<sub>3</sub> following solvent exchange (Table 2 and Figure 2).<sup>33</sup> In

**Table 2.** Experimental and Calculated <sup>1</sup>H NMR Shifts of (*E*)-**2a** and (*E*)-**2a**·ZnCl<sub>2</sub>

H	( <i>E</i> )- <b>2a</b>		( <i>E</i> )- <b>2a</b> ·ZnCl <sub>2</sub>		( <i>E</i> )- <b>2a</b> ·ZnCl <sub>2</sub> *
	expt <sup>a</sup>	calcd <sup>b</sup>	expt <sup>a,c</sup>	calcd <sup>b</sup>	calcd <sup>b</sup>
H <sub>a</sub>	5.46	5.66	5.56	6.26	6.48
H <sub>b</sub>	6.99–7.02	6.94	7.32–7.35	7.25	7.39
H <sub>c</sub>	7.33–7.35	7.47	7.63–7.64	7.29	8.06
H <sub>d</sub>	7.54–7.57	7.53	7.83–7.87	7.69	7.88
H <sub>e</sub>	8.42–8.44	8.59	8.85–8.89	8.82	8.37

<sup>a</sup><sup>1</sup>H NMR (500 MHz, CDCl<sub>3</sub>) data. <sup>b</sup>Calculated <sup>1</sup>H NMR shifts by B3LYP/BSII//B3LYP/BSI computational studies. <sup>c</sup>(*E*)-**2a** (1.0 equiv) and ZnCl<sub>2</sub> (1.0 equiv) in CDCl<sub>3</sub>.

addition, multiple conformations of TBS-silyl ketene acetals (*E*)-**2a**, (*E*)-**2a**·ZnCl<sub>2</sub> (six-membered chelate), (*E*)-**2a**·ZnCl<sub>2</sub>\* (four-membered chelate) were optimized and analyzed (B3LYP/BSII//B3LYP/BSI) to identify low energy conformations for each and provide calculated <sup>1</sup>H NMR chemical

shifts. The observed chemical shifts for the complex formed between (*E*)-**2a** and ZnCl<sub>2</sub> are most consistent with formation of a six-membered chelate (*E*)-**2a**·ZnCl<sub>2</sub> versus a four-membered chelate (Figure 2). In particular, the predicted chemical shifts of H<sub>c</sub> and H<sub>e</sub> for the six-membered chelate are significantly closer to the experimental data. Notably, the calculations for the four-membered chelate (*E*)-**2a**·ZnCl<sub>2</sub>\* predict an *upfield* shift for H<sub>c</sub> compared to (*E*)-**2a**, whereas for the six-membered chelate a *downfield* shift for H<sub>c</sub> is predicted. To further corroborate the energetically favored formation of the six-membered chelate (*E*)-**2a**·ZnCl<sub>2</sub> versus the four-membered chelate, calculations found this complex to be lower in energy by 1.6 kcal/mol. While it is commonly assumed that silyl ethers are unable to coordinate for effective Cram-type chelation during additions to  $\alpha$ -silyloxy carbonyls,<sup>34</sup> recent studies by Walsh with alkyl and vinylzinc reagents are consistent with chelation-controlled addition to  $\alpha$ -silyloxy aldehydes and ketones.<sup>35</sup>

Additional studies support the existence and importance of forming the pre-complexed thiopyridyl ketene acetal (*E*)-**2a**·ZnCl<sub>2</sub> followed by subsequent addition of the aldehyde. Hereafter, these conditions are referred to as *pre-coordination conditions*. Despite the low solubility of ZnCl<sub>2</sub> in CH<sub>2</sub>Cl<sub>2</sub>,<sup>36</sup> we found that mixing an equimolar amount of ZnCl<sub>2</sub> and thiopyridyl ketene acetal (*E*)-**2a** in CH<sub>2</sub>Cl<sub>2</sub> resulted in a nearly homogeneous solution after 10 h (~0.07 M) while the (*Z*)-ketene acetal **2a** required only 5 h to reach homogeneity. In contrast, mixing an equimolar amount of ZnCl<sub>2</sub> and thiophenyl ketene acetal (*E*)-**8a** or pyridine in CH<sub>2</sub>Cl<sub>2</sub> did not generate a homogeneous solution at a similar concentration. These effects were substantiated, as described above, by significant shifts of the protons of the thiopyridyl ring in the <sup>1</sup>H NMR (500 MHz) spectrum of a 1:1 mixture of thiopyridyl ketene acetal (*E*)-**2a** and ZnCl<sub>2</sub> (Figure 2a) in comparison to pure ketene acetal (*E*)-**2a** (Figure 2b, in CDCl<sub>3</sub>).<sup>37</sup> Furthermore, the reaction of pre-coordinated (*E*)-**2b**·ZnCl<sub>2</sub> and hydrocinnamaldehyde **1a** in CH<sub>2</sub>Cl<sub>2</sub> was monitored by aliquot <sup>1</sup>H NMR analysis (following solvent exchange to CDCl<sub>3</sub>) and showed the production of  $\beta$ -lactone **3a** with simultaneous production of TESCl (Scheme 5); however, the  $\beta$ -lactones were generated with greatly diminished diastereoselectivity compared to normal conditions (cf. Table 1, entry 10). In contrast, diminished diastereoselectivity was not observed employing pre-coordination conditions with (*Z*)-**2b**·ZnCl<sub>2</sub> compared to normal conditions (cf. Table 1, entry 11).

The impact of pre-coordination conditions was further demonstrated during the TMAL reaction of 7-trimethylsilyl-5-heptenal **1c**<sup>38</sup> with (*Z*)-**2b**·ZnCl<sub>2</sub> pointing to formation of a kinetically stable Zn(II)–thiopyridyl ketene acetal complex under these conditions (Scheme 6). Use of ketene acetal (*Z*)-**2b** under normal TMAL conditions (i.e., without pre-complexation to ZnCl<sub>2</sub>) gave only a trace amount of  $\beta$ -lactone **3c** while the major product resulted from facile, Lewis acid-mediated, intramolecular cyclization of the allylsilane to the pendant aldehyde leading to vinyl cyclopentane **14**. We predicted that precoordination of ZnCl<sub>2</sub> with ketene acetal (*Z*)-**2b** would lead to

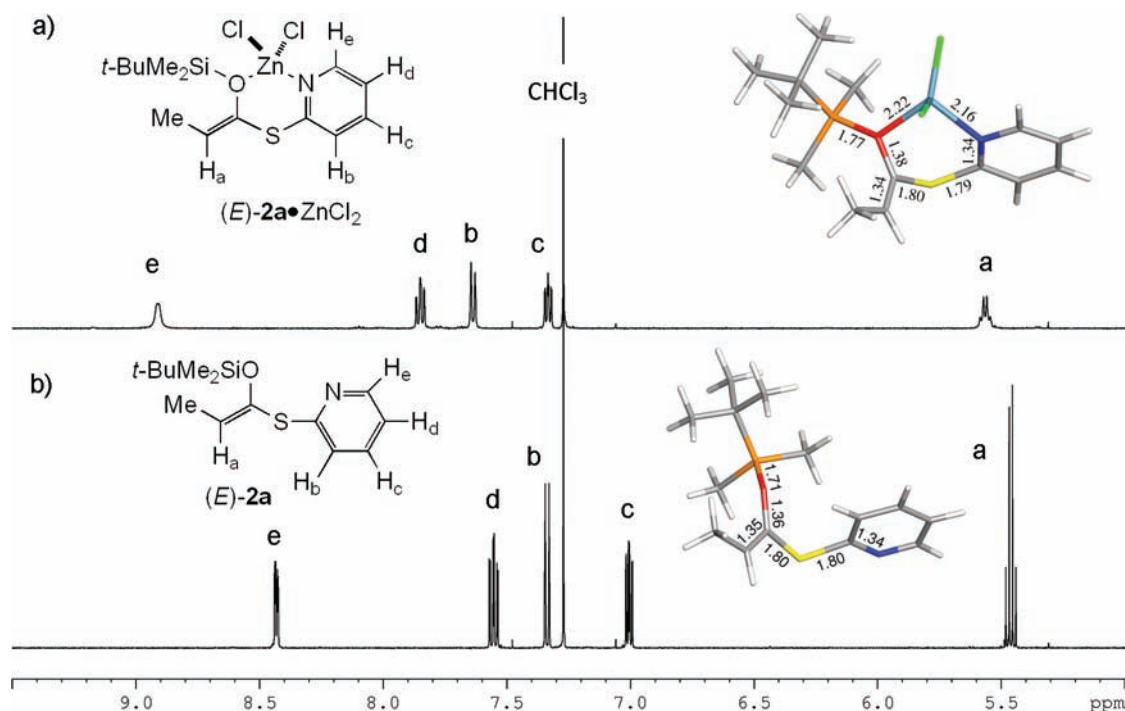
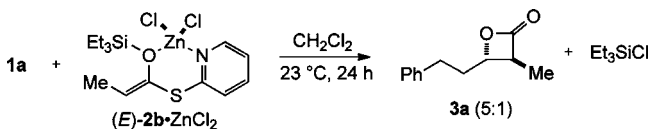
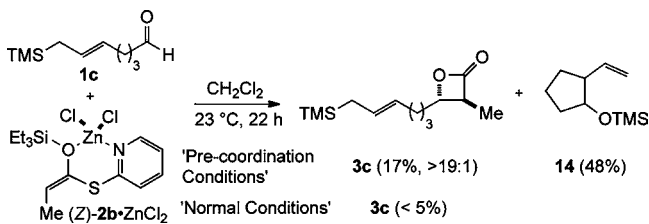


**Figure 2.** B3LYP/BSI-optimized structures accompanied by  $^1\text{H}$  NMR spectra (500 MHz,  $\text{CDCl}_3$ ) of thiopyridyl ketene acetal (*E*)-**2a** (a) with 1.0 equiv of  $\text{ZnCl}_2$  and (b) without  $\text{ZnCl}_2$ . The minor peaks in the aromatic region of (a) are presumably due to the corresponding  $\text{ZnCl}_2$ -complexed thiopyridyl ester from desilylation of ketene acetal (*E*)-**2a**.

**Scheme 5. Detrimental Effect of Pre-coordination Conditions on the Reaction of Hydrocinnamaldehyde **1a** and (*E*) Geometrical Isomer of Ketene Acetal **2b****



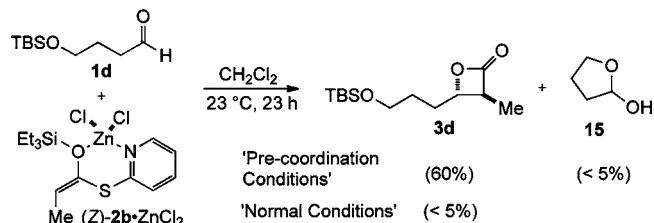
**Scheme 6. A TMAL Process Rendered Competitive with an Intramolecular Allylsilane Cyclization under Pre-coordination Conditions**



reduced Lewis acidity and facilitate access to a productive TMAL process. Indeed, while cyclopentane **14** remained the major product (48%), pre-coordination conditions gave  $\beta$ -lactone **3c** in 17% yield with the typically observed high diastereoselectivity ( $\text{dr} >19:1$ ) for the *trans*- $\beta$ -lactone. Thus, pre-coordination conditions enabled an intermolecular TMAL process (**1c** + (*Z*)-**2b**- $\text{ZnCl}_2$   $\rightarrow$  **3c**) to be competitive with a facile Lewis acid-mediated, intramolecular cyclization (**1c**  $\rightarrow$  **14**).

A more practical example of the utility of pre-coordination conditions was observed during the TMAL reaction of 4-*tert*-butyldimethylsilyloxybutanal **1d**<sup>39</sup> (Scheme 7). When this aldehyde was treated with thiopyridyl ketene acetal (*Z*)-**2b** under normal TMAL conditions, none of the  $\beta$ -lactone **3d** was generated and the major product was lactol **15**<sup>40</sup> again derived

**Scheme 7. Beneficial Effect of Pre-coordination Conditions for the TMAL Process with 4-*tert*-Butyldimethylsilyloxybutanal **1d****



from a facile intramolecular cyclization. When pre-coordination conditions were utilized, the  $\beta$ -lactone **3d** was isolated in good yield with <5% yield of lactol **15** once again pointing to the stability of the (*Z*)-**2b**- $\text{ZnCl}_2$  complex and the utility of these conditions.

**Evidence for a Silylated  $\beta$ -Lactone Intermediate in the TMAL Process.** We previously proposed the intermediacy of a silylated  $\beta$ -lactone intermediate **5** (cf. Figure 1) in the TMAL process.<sup>8</sup> Tetrahydrofuran **16**, isolated under normal conditions with ketene acetal (*Z*)-**2a** following mild base treatment to cleave the corresponding silyl ester,<sup>8a</sup> is likely generated by cyclization of the pendant silyloxy moiety with the silylated  $\beta$ -lactone **5** generated during the TMAL process (Scheme 8).<sup>41</sup> This result sheds some light on the lack of  $\beta$ -lactone **3d** observed under “normal” conditions (cf. Scheme 7) since the small quantity of  $\beta$ -lactone **3d** that does form is most likely opened to afford THF **16**, likely aided by the action of uncomplexed  $\text{ZnCl}_2$ . We previously reported that the size of the silyl group of thiopyridyl ketene acetals **2** significantly impacted isolated yields of  $\beta$ -lactones<sup>8b</sup> with less bulky silyl groups (i.e., TES and TBS) providing higher yields versus larger silyl groups (i.e., TIPS) (Table 3). The major byproducts isolated with

**Scheme 8. Isolation of Tetrahydrofuran Byproduct 16 from 4-*tert*-Butyldimethylsilyoxybutanal 1d and Ketene Acetal (Z)-2a Indicative of a Silylated  $\beta$ -Lactone Intermediate 5**

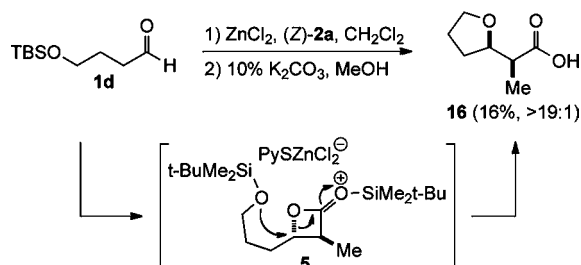
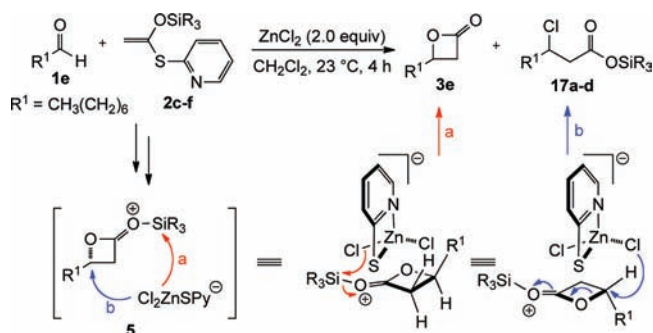


**Table 3. Effect of the Silyl Group of Thiopyridyl Ketene Acetals 2c–f on the TMAL Reaction**



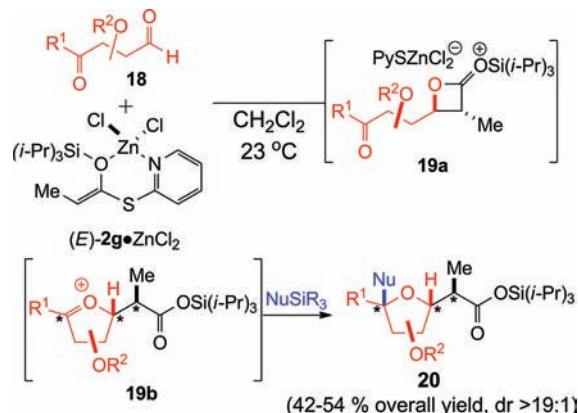
entry	$\text{SiR}_3$ ( <b>2</b> )	<b>3e</b> % yield	<b>17</b> % yield
1	TES ( <b>2c</b> )	66 <sup>a</sup>	<5 <sup>b</sup> ( <b>17a</b> )
2	TBS ( <b>2d</b> )	53 <sup>a</sup>	8 <sup>b</sup> ( <b>17b</b> )
3	TIPS ( <b>2e</b> )	20 <sup>a</sup>	40 <sup>b</sup> ( <b>17c</b> )
4	TBDPS ( <b>2f</b> )	<5 <sup>c</sup>	56 <sup>a</sup> ( <b>17d</b> )

<sup>a</sup>Refers to isolated yields. <sup>b</sup>Estimated based on crude  $^1\text{H}$  NMR analysis. <sup>c</sup>Not detected based on crude  $^1\text{H}$  NMR (300 MHz) analysis.

bulky silyl groups were  $\beta$ -chlorosilyl esters **17a–d**, reasonably derived from intermolecular cleavage of the silylated  $\beta$ -lactone intermediate **5** by chloride ion. This process was previously optimized for the synthesis of a *trans*- $\beta$ -chlorosilyl ester using a  $\text{SnCl}_4$ -mediated TMAL reaction proposed to proceed through a silylated *cis*- $\beta$ -lactone.<sup>13</sup> In a similar manner, use of a TBDPS-ketene acetal in the  $\text{ZnCl}_2$ -mediated TMAL process leads to near exclusive formation of a  $\beta$ -chlorosilyl ester **17d** (Table 3, entry 4).<sup>23a</sup> Thus, a partitioning between desilylation leading to a  $\beta$ -lactone product (pathway a) or chloride cleavage leading to a  $\beta$ -chlorosilyl ester (pathway b) that depends on the steric size of the silyl group provides further evidence for the silylated  $\beta$ -lactone intermediate **5**.

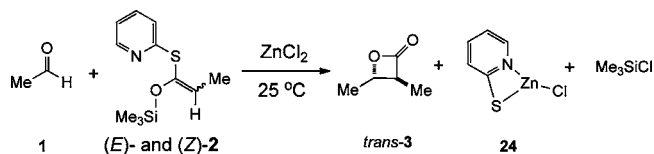
The discovery of pre-coordination conditions (cf. (E)-**2**- $\text{ZnCl}_2$ ) and silylated  $\beta$ -lactone intermediates in the TMAL process was exploited by the development of a novel cascade, three-component synthesis of tetrahydrofurans<sup>23</sup> and tetrahydropyrans<sup>24</sup> from ketoaldehydes via the TMAL process (Scheme 9). This cascade sequence capitalized on the expected reactivity at the C4 carbon of the silylated  $\beta$ -lactone intermediate **19a** toward substitution by a pendant ketone<sup>23b</sup> and a derived cyclic oxocarbenium **19b** that could undergo subsequent nucleophilic addition by silane nucleophiles. This three-component coupling involving a ketoaldehyde, a thiopyridyl ketene acetal, and a silane nucleophile was applied to a concise synthesis of the tetrahydrofuran fragment of colopsinol B.<sup>23a</sup>

**Scheme 9. Cascade Process toward the Synthesis of Tetrahydrofurans and Tetrahydropyrans Premised on the Silylated  $\beta$ -Lactone Intermediate**



**Mechanistic Proposal for the  $\text{ZnCl}_2$ -Mediated TMAL Reaction of Achiral Aldehydes and Thiopyridyl Ketene Acetals Garnered from B3LYP/BSI Calculations: Asynchronous Concerted, Boatlike Transition-State Arrangements *en Route* to Functional Silylated  $\beta$ -Lactone Intermediates.** Computational studies (B3LYP/BSI) were performed to locate possible intermediates and transition states for the various steps proposed for the TMAL mechanism using both isomeric ketene acetals, (E)-**2** and (Z)-**2**, leading to thiopyridyl- $\text{ZnCl}_2$  complex **24**, *trans*- $\beta$ -lactone **3**, and  $\text{Me}_3\text{SiCl}$  (Scheme 10). To simplify the calculations, a trimethylsilyl

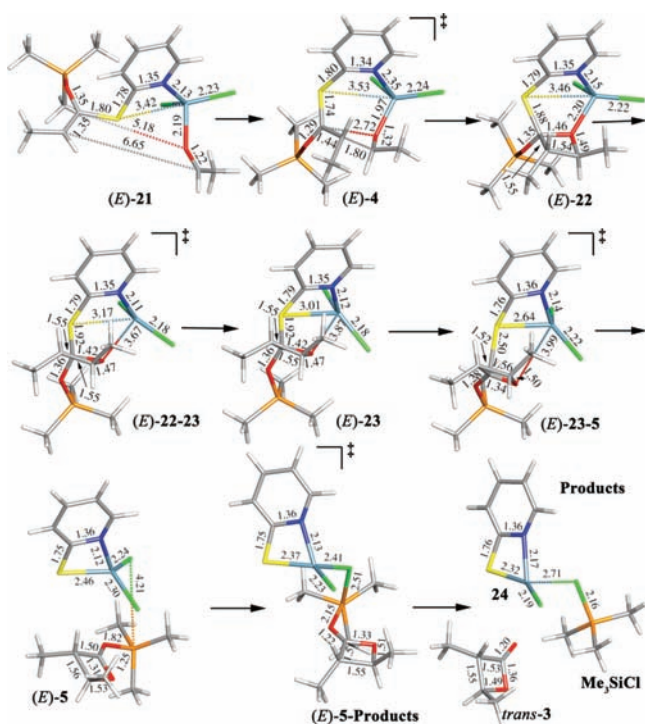
**Scheme 10. Hypothetical TMAL Process Studied by B3LYP/BSI Calculations**



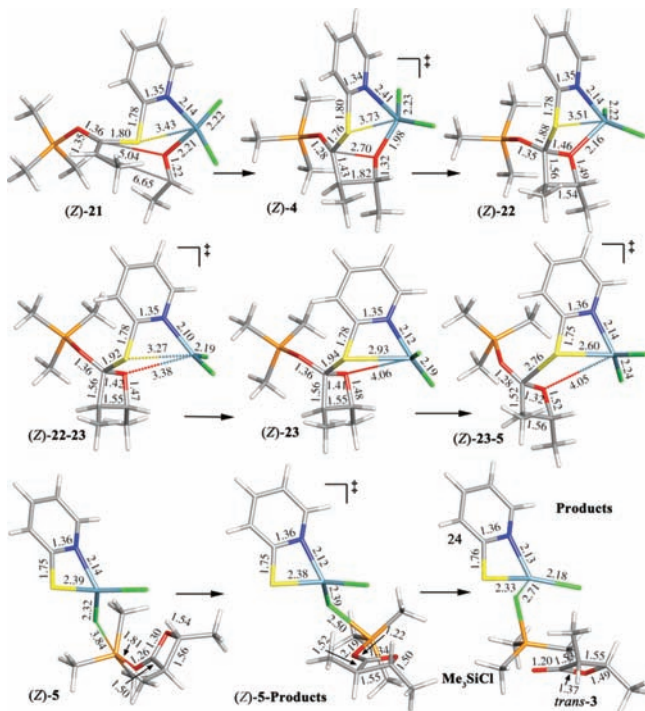
group was used rather than the typical experimentally employed triethyl or TBS groups for the ketene acetal. Structural details of both *E* and *Z* pathways can be found in Figures 3 and 4, respectively, and the overall energy profile of the TMAL pathways for both ketene acetal geometries is shown in Figure 5. Note that only the lowest energy conformations (E Conf1 and Z Conf2) for the (E)- and (Z)-ketene acetal reaction profiles are shown.<sup>42</sup>

Following complexation of both the thiopyridyl ketene acetal (E)-**2** and aldehyde **1** to  $\text{ZnCl}_2$  which are calculated to be energetically favorable (Figure 5), computational studies indicate that formation of oxetane (E)-**22** involves a concerted but asynchronous formation of both the C–O and C–C bond via transition state (E)-**4** (i.e., (E)-**21-22**),<sup>43</sup> with a  $\Delta H^\ddagger$  ( $\Delta G^\ddagger$ ) barrier of 23.48 kcal/mol (30.57 kcal/mol) and an imaginary mode of 187.2i  $\text{cm}^{-1}$ . Formation of the oxetane (E)-**22** is slightly endothermic (endergonic) being 0.15 kcal/mol (7.63 kcal/mol) higher in enthalpy (free energy) than the aldehyde- $\text{ZnCl}_2$ -thiopyridyl ketene acetal complex (E)-**21**. After formation of oxetane (E)-**22**, the Zn–O (formerly aldehyde O) bond is broken via transition state (E)-**22-23** to form intermediate (E)-**23** with a  $\Delta H^\ddagger$  ( $\Delta G^\ddagger$ ) barrier of 6.97 (6.34) kcal/mol and a small imaginary mode of 13.2i  $\text{cm}^{-1}$ . From



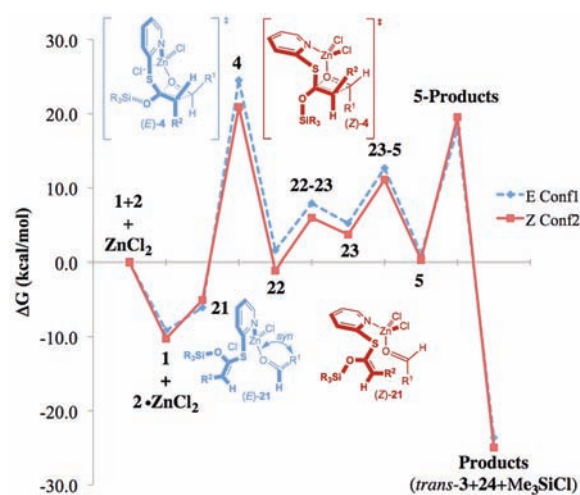


**Figure 3.** Calculated structures (B3LYP/BSI) for intermediates and transition states of the TMAL process for the (*E*)-ketene acetal 2 pathway leading to *trans*- $\beta$ -lactone 3.



**Figure 4.** Calculated structures (B3LYP/BSI) for intermediates and transition states for the TMAL process of the (*Z*)-ketene acetal 2 pathway leading to *trans*- $\beta$ -lactone 3.

(*E*)-22 to (*E*)-23 the Zn–O bond distance increases from 2.20 to 3.87 Å. In addition to the Zn–O bond breaking, the Zn–S bond distance decreases from 3.46 to 3.01 Å. Intermediate (*E*)-23 is 7.41 (3.63) kcal/mol higher in energy compared to (*E*)-22.<sup>44</sup> After cleavage of the Zn–O bond, the S–C

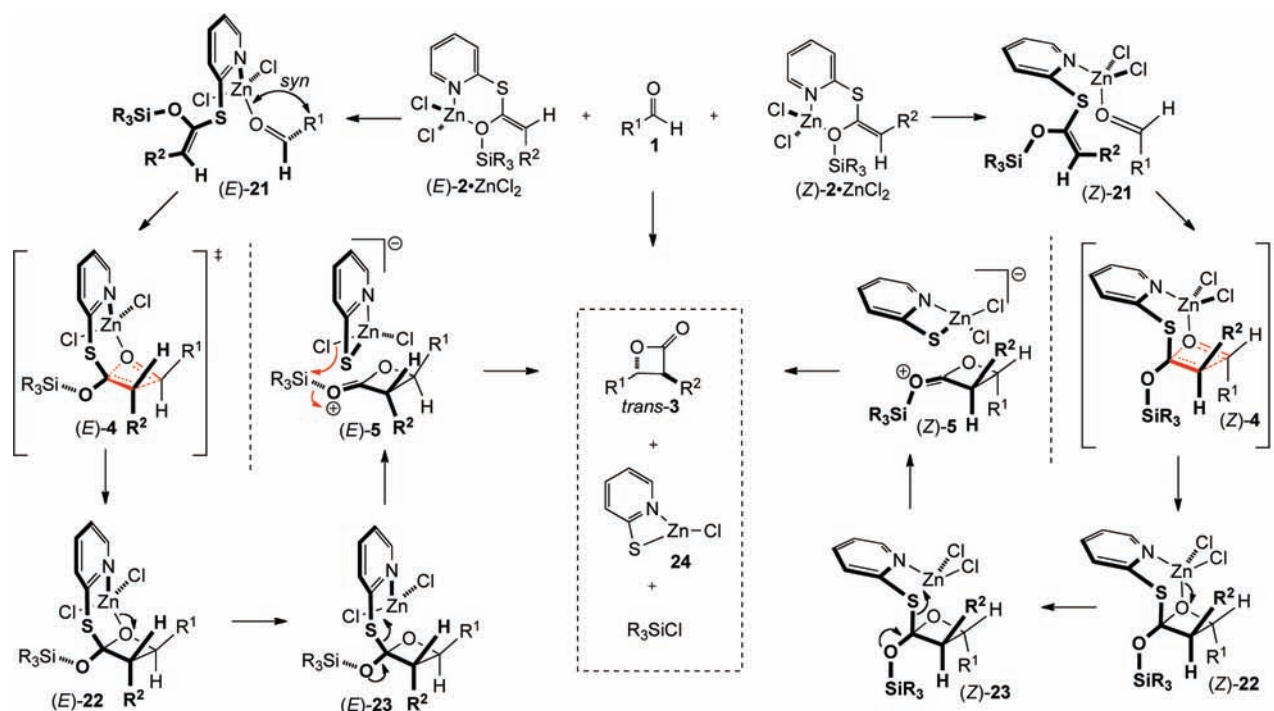


**Figure 5.** Reaction profile for the TMAL reaction with calculated (B3LYP/BSI) Gibbs free energy values ( $\Delta G$ ).

bond breaks, increasing from 1.92 to 3.96 Å, with a  $\Delta H^\ddagger$  ( $\Delta G^\ddagger$ ) barrier of 5.56 (7.47) kcal/mol to form the silylated  $\beta$ -lactone intermediate (*E*)-5. The transition state, (*E*)-23-5, has an imaginary mode of 95.2i  $\text{cm}^{-1}$ . During scission of the S–C bond, the Zn–S bond distance decreases from 3.01 Å in (*E*)-23 to 2.46 Å in (*E*)-5. The last step in the mechanism involves chloride ion addition to silicon giving a pentacoordinate silicate and ultimately providing *trans*- $\beta$ -lactone 3, Zn(II)-SPY complex 24, and  $\text{Me}_3\text{SiCl}$  with a  $\Delta H^\ddagger$  ( $\Delta G^\ddagger$ ) barrier of 15.69 (16.91) kcal/mol. The transition state for desilylation, (*E*)-5-products, has an imaginary mode of 147.5i  $\text{cm}^{-1}$ . The  $\beta$ -lactone 3 and byproducts are 3.20 (24.65) kcal/mol downhill in energy from (*E*)-5. In summary, the rate-limiting step for the reaction of (*E*)-21 to the products (*trans*-3, 24, and  $\text{Me}_3\text{SiCl}$ ) is calculated to be the first step ((*E*)-21 to (*E*)-22) involving a concerted, asynchronous formation of the oxetane with a  $\Delta H^\ddagger$  ( $\Delta G^\ddagger$ ) barrier of 23.48 (30.57) kcal/mol and the  $\Delta H_{\text{rxn}}$  ( $\Delta G_{\text{rxn}}$ ) from (*E*)-21 to the products is calculated to be exothermic (exergonic) by 3.20 (24.65) kcal/mol.

The TMAL process for the (*Z*)-ketene acetal 21 follows a reaction path nearly identical to that for the (*E*)-ketene acetal 21. The most notable difference between these two reaction pathways is the rate-limiting step, (*Z*)-21  $\rightarrow$  (*Z*)-22, which is 4.41 (4.61) kcal/mol lower in enthalpy (free energy) for the (*Z*)- compared to the (*E*)-ketene acetal. These computational studies are consistent with faster reaction rates qualitatively observed for the (*Z*)- vs (*E*)-ketene acetals since the former avoids development of an unfavorable, eclipsing interaction between the  $\text{R}^1$  group of the aldehyde and the  $\text{R}^2$  group of the ketene acetal in the transition state (*vide infra*).

To determine if a larger  $\text{R}^3$  group (silicon substituent) would have a significant effect on the rate-limiting step, the first step of the reaction mechanism involving (*E*)-ketene acetal 21 was calculated with  $\text{R}^1 = \text{R}^2 = \text{Me}$  and  $\text{R}^3 = t\text{-BuMe}_2$  and the activation energy decreased by less than 3 kcal/mol compared to the TMS ketene acetal. To investigate the importance of the sulfur atom, the rate-limiting step was recalculated with oxygen replacing sulfur, an oxopyridyl ketene acetal, and with carbon replacing sulfur with the previously employed substrates ( $\text{R}^1 = \text{R}^2 = \text{Me}$ ;  $\text{R}^3 = \text{Me}_3$ ). The activation barriers for the oxo and carbon ketene acetals were calculated to be within 4 kcal/mol of the sulfur-containing model. These results lead us to

Scheme 11. Overall Mechanistic Proposal for the ZnCl<sub>2</sub>-Mediated TMAL Reaction of Achiral Aldehydes and Both (*E*)- and (*Z*)-Thiopyridyl Ketene Acetals<sup>a</sup>

<sup>a</sup>To simplify comparison, enantiomeric structures are shown for the (*Z*) pathway.

conclude that the sulfur atom was not absolutely critical to the success of the TMAL process.

The proposed overall mechanism for the TMAL process based on the combination of experimental and computational data collected to date is presented in Scheme 11. Initially, two distinct tetrahedral zinc(II)–thiopyridyl ketene acetal complexes (*E*)- and (*Z*)-2·ZnCl<sub>2</sub>, involving coordination of ZnCl<sub>2</sub> to both the pyridine nitrogen and silylether oxygen of the ketene acetal, are supported by both calculations and <sup>1</sup>H NMR studies presented herein (cf. Table 2 and Figure 2). The lowest energy conformations of these complexes, as determined by calculations, are in agreement with pinwheel conformations of ketene acetals previously described by Wilcox for similar *O*-alkyl silylketene acetals.<sup>45</sup> Upon addition of aldehyde **1**, exchange of the silyl ether oxygen for the aldehyde occurs to form diastereomeric tetrahedral zinc(II) complexes (*E*)- and (*Z*)-21. Four-coordinate zinc(II) complexes with tetrahedral geometry are the most common<sup>46</sup> and several pseudorotation and dissociation/re-coordination pathways that are not discussed or shown may be necessary in order to access the productive complexes (*E*)- and (*Z*)-21.<sup>47</sup> There is a distinct energetic difference between these two diastereomeric transition-state arrangements leading to the asynchronous, concerted C–C and C–O bond-forming events that generate the oxetane intermediates (*E*)- and (*Z*)-22. An unfavorable *syn* coordination of the aldehyde to Zn(II) is required for (*E*)-21 but not (*Z*)-21 to access the reactive conformation for oxetane formation. MP2/6-31G\* calculations suggest that *anti* coordination of BF<sub>3</sub>·acetaldehyde is favored over *syn* coordination by 1.22 kcal/mol and an *anti*-BF<sub>3</sub>·benzaldehyde complex was estimated to be 5.31 kcal/mol more stable than the corresponding *syn* complex.<sup>48</sup> In line with these reports, we found that (*Z*)-2b provided higher diastereoselectivity than (*E*)-2b with hydrocinnamaldehyde under precoordination conditions (cf. Scheme 5)

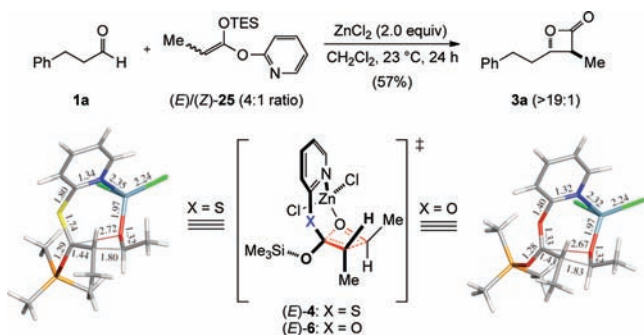
and complete stereodivergent diastereoselectivity was observed with *p*-nitrobenzaldehyde, likely due to the high energy barrier required for *syn* coordination, to provide *cis*-β-lactone (cf. Scheme 3).<sup>6</sup> An asynchronous concerted, boat-like transition state is proposed leading to formation of oxetanes (*E*)- and (*Z*)-22. We suggest that cleavage of the Zn–O bond followed by S–C bond cleavage releases ring strain providing a driving force leading to diastereomeric silylated β-lactone intermediates (*E*)- and (*Z*)-5. Stable bidentate chelation with S and N,<sup>32</sup> between the liberated zinc and the thiopyridyl prevents release from the thiopyridyl dichlorozincate and instead leads to chloride induced desilylation to deliver β-lactone **3** and thiopyridyl zinc monochloride **24**. Consideration of bond strengths (Zn–S, 50.0 kcal/mol; Zn–Cl, 54.7 kcal/mol)<sup>49</sup> and results with thiophenyl ketene acetals **8a,b** (cf. Table 1, entries 6–9, and Scheme 4) lend further evidence for the stability of Zn(II)–SPy complexes leading to the bidentate dichlorozincate intermediate (*E*)-5. In contrast, when thiophenyl ketene acetals **8a,b** were utilized, no β-chlorosilyl ester byproducts (cf. Table 3) were observed as with the use of thiopyridyl ketene acetals but rather β-thiophenyl silylestere (cf. Scheme 4) were produced demonstrating a Zn(II) affinity trend of PhS<sup>−</sup> > Cl<sup>−</sup> > PyS<sup>−</sup> pointing to the importance of the thiopyridyl moiety for the highest yield of β-lactones. Formation of the bidentate chelate **24** also prevents generation of a silyl pyridyl sulfide (PySSiR<sub>3</sub>) that may be responsible for silicon-catalyzed aldol products as observed in the TMAL reaction of thiophenyl ketene acetals.<sup>50</sup> We propose that tetrahydrofurans (THFs), tetrahydropyrans (THPs), and β-chlorosilyl esters (cf. Table 3, Schemes 8 and 9) are all derived from competitive, invertive alkyl C–O ring scission of the silylated β-lactone intermediate (*E*)- and (*Z*)-5 as opposed to intermolecular desilylation by chloride ion which delivers *trans*-β-lactone **3**. This result also correlates to the finding that more readily cleaved, less bulky silyl groups (e.g.,



TES or TBS) provide higher yields of  $\beta$ -lactone **3** (cf. Table 3). In contrast, larger silyl groups (i.e., TIPS or TBDPS) divert nucleophilic attack of chloride ion to the  $\beta$ -carbon of the silylated  $\beta$ -lactone intermediate **5**, leading to higher yields of  $\beta$ -chloro silyl esters. The stereochemical outcome of the C–O cleavage leading to THFs and THPs<sup>23,24</sup> (cf. Scheme 9) and characterization of the isolable *tert*-butyldiphenylsilyl ester **14d** (cf. Table 3, entry 4) supports an S<sub>N</sub>2-like, invertive alkyl C–O ring scission. Finally, these mechanistic proposals are consistent with our finding that the ZnCl<sub>2</sub>-mediated TMAL reaction with thiopyridyl ketene acetals **2** is stoichiometric while the same reaction employing thiophenyl ketene acetals **8** is catalytic in ZnCl<sub>2</sub>.

**Development of an Oxopyridyl Ketene Acetal-Based TMAL Process.** The predictive power of a mechanistic proposal is its greatest value. Our described experiments and calculations leading to the described mechanistic model for the TMAL process, suggested that an oxopyridyl ketene acetal (e.g., (*E*)-**25**) would also participate in a TMAL process since the sulfur atom of thiopyridyl ketene acetals does not coordinate to zinc in the rate limiting-step. This prediction was indeed corroborated by experiment. As seen in Scheme 12, reasonable

**Scheme 12. Synthesis of  $\beta$ -Lactone **3a** from Oxopyridyl Ketene Acetal (*E*)-**25** and Comparison of Transition States for Thio- versus Oxopyridyl Ketene Acetals**



yield (57%) and high diastereoselectivity was obtained using oxopyridyl ketene acetals (*E*)/(*Z*)-**25** (4:1 ratio) with hydrocinnamaldehyde (cf. Table 1, entry 10; 70% yield with thiopyridyl ketene acetal) under similar reaction conditions. The reaction is also stereoconvergent with respect to ketene acetal geometry as expected. The slightly decreased yield compared to the thiopyridyl ketene acetal (*E*)-**2b** suggests that the sulfur atom may play some role toward maximum conversion. Despite the large difference in bond lengths between the C–S and C–O bonds (1.80 vs 1.40 Å; 1.74 vs 1.33 Å), a similar transition-state arrangement is observed for both reactions (Scheme 12, only (*E*)-ketene acetal transition state shown). This variation in bond lengths is accommodated by a more acute C–S–C bond angle, which leads to nearly identical bond lengths for the forming C–C bond (1.80 vs 1.83 Å) in the two transition states.

## CONCLUSIONS

The tandem Mukaiyama aldol lactonization (TMAL) reaction of aldehydes and thiopyridyl ketene acetals provides a highly diastereoselective approach to a variety of *trans*-1,2-disubstituted  $\beta$ -lactones. Through both experimental and theoretical studies, we demonstrated that coordination of the nitrogen of the thiopyridyl group with Zn(II) plays a crucial role in

the TMAL reaction and suggests that it is responsible for the high efficiency and diastereoselectivity of this process. This critical interaction was further supported by calculations that show strong evidence for an asynchronous concerted, boat-like transition-state arrangement. This mechanistic proposal provides plausible rationalizations for the unique features of the TMAL reaction including the absence of a *gem*-dialkyl effect and the fact that typical aldol products are not produced. Calculations and further experiments support the existence of a silylated  $\beta$ -lactone intermediate, which was previously proposed and utilized in novel multi-component processes involving the TMAL process.<sup>23a,24</sup> Finally, as a demonstration of the utility of the calculations and mechanistic proposals described herein, an oxo version of the TMAL process was proposed and, as predicted, was found to provide similar yields and diastereoselectivity to the thiopyridyl analogue.

## ASSOCIATED CONTENT

### Supporting Information

Experimental details and characterization data for (*Z*)-thiopyridyl ketene acetal **2b**,  $\beta$ -lactones **3c-d**, thiophenyl ketene acetal **8a**, aldol adducts **9a,b** and **10a,b**, thioacetal **11b**,  $\beta$ -thiophenyl methyl ester **13**, oxopyridyl ester **S1**, and oxopyridyl ketene acetal **25**; NMR studies; computational details; and ancillary calculations. This material is available free of charge via the Internet at <http://pubs.acs.org>.

## AUTHOR INFORMATION

### Corresponding Author

romo@tamu.edu; mouse@tamu.edu; mitchell@ilstu.edu

### Present Addresses

<sup>†</sup>Sundia MedTech Co., Ltd., 332 Adiseng Rd., Zhangjiang Hi-Tech Park, Shanghai 201203

## ACKNOWLEDGMENTS

Support of this work by the NSF (CHE 0809747) and the Robert A. Welch Foundation (A-1280) is gratefully acknowledged. We thank Prof. Dan Singleton (Texas A&M), Dr. Hong Woon Yang (Array Biopharma), and Dr. Yingcai Wang (Amgen) for helpful discussions and Mr. Alfred Tuley for resynthesis of thiopyridyl ketene acetal (*E*)-**2a**. We thank the Supercomputing Facility at Texas A&M University for providing computer time and NSF (CHE-0541587). Mass spectral analyses were obtained at the Texas A&M Center for Chemical Characterization and Analysis on instruments acquired by generous funding from the NSF (CHE-8705697) and the TAMU Board of Regents Research Program. The NSF (CHE-0416260, TAMU; CHE-0722385, ISU) also provided funds for purchase of NMR instrumentation.

## REFERENCES

- (1) For reviews describing  $\beta$ -lactones in the context of natural products, see: (a) Wang, Y.; Tennyson, R. L.; Romo, D. *Heterocycles* **2004**, *64*, 605–658. (b) Lowe, C.; Vederas, J. C. *Org. Prep. Proced. Int.* **1995**, *27*, 305–346. For reviews describing stereoselective  $\beta$ -lactone synthesis and their utility, see: (c) Yang, H. W.; Romo, D. *Tetrahedron* **1999**, *55*, 6403–6434. (d) Pommier, A.; Pons, J.-M. *Synthesis* **1995**, 729–744. (e) Pommier, A.; Pons, J.-M. *Synthesis* **1993**, 441–449. For selected recent methods for  $\beta$ -lactone synthesis, see: (f) Merlic, C. A.; Doroh, B. C. *J. Org. Chem.* **2003**, *68*, 6056–6059. (g) Nelson, S. G.; Zhu, C.; Shen, X. *J. Am. Chem. Soc.* **2004**, *126*, 14–15. (h) Wilson, J. E.; Fu, G. C. *Angew. Chem., Int. Ed.* **2004**, *43*, 6358–6360. (i) Getzle, Y. D. Y. L.; Kundnani, V.; Lobkovsky, E. B.; Coates, G. W. *J. Am. Chem.*

- Soc. **2004**, *126*, 6842–6843. (j) Zhu, C.; Shen, X.; Nelson, S. G. *J. Am. Chem. Soc.* **2004**, *126*, 5352–5253. (k) Calter, M. A.; Tretyak, O. A.; Flaschenriem, C. *Org. Lett.* **2005**, *7*, 1809–1812. (l) Oh, S.; Cortez, G. S.; Romo, D. *J. Org. Chem.* **2005**, *70*, 2835–2838. (m) Henry-Riyad, H.; Lee, C.; Purohit, V. C.; Romo, D. *Org. Lett.* **2006**, *8*, 4363–4366. (n) Reddy, L. R.; Corey, E. J. *Org. Lett.* **2006**, *8*, 1717–1719. (o) Cho, S. W.; Romo, D. *Org. Lett.* **2007**, *9*, 1537–1540. (p) Ma, G.; Nguyen, H.; Romo, D. *Org. Lett.* **2007**, *9*, 2143–2146. (q) Kull, T.; Peters, R. *Angew. Chem., Int. Ed.* **2008**, *47*, 5461–5464. (r) He, L.; Lv, H.; Zhang, Y. R.; Ye, S. *J. Org. Chem.* **2008**, *73*, 8101–8103. (s) Wang, X.-N.; Shao, P.-L.; Lv, H.; Ye, S. *Org. Lett.* **2009**, *11*, 4029–4031. (t) Chidara, S.; Lin, Y.-M. *Synlett* **2009**, 1675–1679. (u) Mondal, M.; Ibrahim, A. A.; Wheeler, K. A.; Kerrigan, N. J. *Org. Lett.* **2010**, *12*, 1664–1667. (v) Kull, T.; Cabrera, J.; Peters, R. *Chem.—Eur. J.* **2010**, *16*, 9132–9139. (w) Aronica, L. A.; Mazzoni, C.; Caporusso, A. M. *Tetrahedron* **2010**, *66*, 265–273. (x) Morris, K. A.; Arendt, K.; Oh, S.; Romo, D. *Org. Lett.* **2010**, *12*, 3764–3767. (y) Leverett, C. A.; Purohit, V. C.; Romo, D. *Angew. Chem., Int. Ed.* **2010**, *49*, 9479–9483.
- (2) (a) Tidwell, T. T. *Angew. Chem., Int. Ed.* **2005**, *44*, 5778–5785. (b) Tidwell, T. T. *Eur. J. Org. Chem.* **2006**, 563–576.
- (3) Purohit, V. C.; Matla, A. S.; Romo, D. *Heterocycles* **2008**, *76*, 949–979.
- (4) Staudinger, H.; Bereza, S. *Ann.* **1911**, *380*, 243–277.
- (5) Wynberg, H.; Staring, E. G. J. *J. Am. Chem. Soc.* **1982**, *104*, 166–168.
- (6) Hirai, K.; Homma, H.; Mikoshiba, I. *Heterocycles* **1994**, *38*, 281–282.
- (7) Wang, Y.; Zhao, C.; Romo, D. *Org. Lett.* **1999**, *1*, 1197–1999.
- (8) (a) Yang, H. W.; Romo, D. *J. Org. Chem.* **1997**, *62*, 4–5. (b) Yang, H. W.; Zhao, C.; Romo, D. *Tetrahedron* **1997**, *53*, 16471–16488.
- (9) (a) Yang, H. W.; Romo, D. *J. Org. Chem.* **1998**, *63*, 1344–1347. (b) Romo, D.; Harrison, P. H. M.; Jenkins, S. I.; Riddoch, R. W.; Park, K.; Yang, H. W.; Zhao, C.; Wright, G. D. *Bioorg. Med. Chem.* **1998**, *6*, 1255–1272.
- (10) (a) Dollinger, L. M.; Howell, A. R. *J. Org. Chem.* **1998**, *63*, 6782–6783. (b) Yin, J.; Yang, X. B.; Chen, Z. X.; Zhang, Y. H. *Chin. Chem. Lett.* **2005**, *16*, 1448–1450. (c) For a less successful use of the TMAL process, see: Trost, B. M.; Papillon, J. P. N.; Nussbaumer, T. *J. Am. Chem. Soc.* **2005**, *127*, 17921–17937.
- (11) (a) Ma, G.; Zancanella, M.; Oyola, Y.; Richardson, R. D.; Smith, J. W.; Romo, D. *Org. Lett.* **2006**, *8*, 4497–4500. (b) Zhang, W.; Richardson, R. D.; Chamni, S.; Smith, J. W.; Romo, D. *Bioorg. Med. Chem. Lett.* **2008**, *28*, 2491–2494. (c) Richardson, R. D.; Ma, G.; Oyola, Y.; Zancanella, M. A.; Knowles, L. M.; Cieplak, P.; Romo, D.; Smith, J. W. *J. Med. Chem.* **2008**, *51*, 5285–5296.
- (12) Schmitz, W. D.; Messerschmidt, N. B.; Romo, D. *J. Org. Chem.* **1998**, *63*, 2058–2059.
- (13) Wang, Y.; Romo, D. *Org. Lett.* **2002**, *4*, 3231–3234.
- (14) Cho, S. W.; Romo, D. *Org. Lett.* **2007**, *9*, 1537–1540.
- (15) Yang, P.-Y.; Liu, K.; Ngai, M. H.; Lear, M. J.; Wenk, M. R.; Yao, S. Q. *J. Am. Chem. Soc.* **2010**, *132*, 656–666.
- (16) (a) Kridel, S. J.; Axelrod, F.; Rozenkrantz, N.; Smith, J. W. *Cancer Res.* **2004**, *64*, 2070. (b) Knowles, L. M.; Axelrod, F.; Browne, C. D.; Smith, J. W. *J. Biol. Chem.* **2004**, *279*, 30540. (c) Purohit, V. C.; Richardson, R. D.; Smith, J. W.; Romo, D. *J. Org. Chem.* **2006**, *71*, 4549–4558.
- (17) (a) Mukaiyama, T.; Narasaka, K.; Banno, K. *Chem. Lett.* **1973**, 1011–1014. (b) Mukaiyama, T.; Banno, T.; Narasaka, K. *J. Am. Chem. Soc.* **1974**, *96*, 7503–7509. (c) Heathcock, C. H. *Science* **1981**, *214*, 395–400. (d) Mukaiyama, T. *Aldrichimica Acta* **1996**, *29*, 59–76. For selected recent papers describing the continued utility of the Mukaiyama aldol reaction, see: (e) Bolla, M. L.; Patterson, B.; Rychnovsky, S. D. *J. Am. Chem. Soc.* **2005**, *127*, 16044–16045. (f) Cheon, C. H.; Yamamoto, H. *Org. Lett.* **2010**, *12*, 2476–2479. (g) Alam, J.; Keller, T. H.; Loh, T.-P. *J. Am. Chem. Soc.* **2010**, *132*, 9546–9548. (h) Mei, Y.; Dissanayake, P.; Allen, M. J. *J. Am. Chem. Soc.* **2010**, *132*, 12871–12873. (i) Saadi, J.; Akakura, M.; Yamamoto, H. *J. Am. Chem. Soc.* **2011**, *133*, 14248–14251.
- (18) (a) Zimmerman, H. E.; Traxler, M. D. *J. Am. Chem. Soc.* **1957**, *79*, 1920–1923. (b) Palomo, C.; Oiarbide, M.; Garcia, J. M. *Chem.—Eur. J.* **2002**, *8*, 36–44. (c) Geary, L. M.; Hultin, P. G. *Tetrahedron: Asymmetry* **2009**, *20*, 131–173.
- (19) Computational details can be found in the Supporting Information.
- (20) Some of the experimental studies described herein were described previously: Zhao, C. Ph. D. Thesis, Texas A&M University, 2001.
- (21) (a) Allinger, N. L.; Zalkow, V. *J. Am. Chem. Soc.* **1960**, *25*, 701–704. (b) Parrill, A. L.; Dalata, D. P. *Tetrahedron Lett.* **1994**, *35*, 7319–7322. (c) For a review, see: Jung, M. E. *Synlett* **1999**, 843–846.
- (22) (a) Danheiser, R. L.; Nowick, J. S.; Lee, J. H.; Miller, R. F.; Huboux, A. H. *Org. Synth.* **1996**, *73*, 61–72. (b) Wedler, C.; Schick, H. *Org. Synth.* **1998**, *75*, 116–123. (c) Wedler, C.; Ludwig, R.; Schick, H. *Pure Appl. Chem.* **1997**, *69*, 605–608.
- (23) (a) Mitchell, T. A.; Zhao, C.; Romo, D. *Angew. Chem., Int. Ed.* **2008**, *47*, 5026–5029. For related stepwise processes, see: (b) Mead, K. T.; Pillai, S. K. *Tetrahedron Lett.* **1993**, *34*, 6997–7000. (c) Mitchell, T. A.; Romo, D. *J. Org. Chem.* **2007**, *72*, 9053–9059.
- (24) Mitchell, T. A.; Zhao, C.; Romo, D. *J. Org. Chem.* **2008**, *73*, 9544–9551.
- (25) 2-Mercaptopyrindine has served as an invaluable scaffold for many reactions. For a review, see: Schmidt, B.; Kuhn, C. *J. Prakt. Chem.* **1999**, *341*, 114–120.
- (26) More thiophilic Lewis acids, such as HgCl<sub>2</sub>, CdCl<sub>2</sub>, and CuCl<sub>2</sub>, were also studied for their ability to promote a TMAL reaction with thiopyridyl ketene acetals. HgCl<sub>2</sub> and CuCl<sub>2</sub> only led to desilylation of the ketene acetal to the corresponding thiopyridyl ester along with recovered aldehyde and CdCl<sub>2</sub> gave no reaction. In light of these failures, we reason that the accessible geometries of the metal complexes must also play an important role for a successful TMAL reaction. For a discussion of the affinity of transition metals toward sulfur ligands, see: Kuehn, C. G.; Isied, S. S. *Prog. Inorg. Chem.* **1980**, *27*, 153–218.
- (27) For a recent review of dyotropic rearrangements including that of  $\beta$ -lactones, see: Fernandez, I.; Cossio, F. P.; Sierra, M. A. *Chem. Rev.* **2009**, *109*, 6687–6711.
- (28) We considered that a zinc enolate could be formed in the TMAL by transmetalation of the thiopyridyl ketene acetal, but independent generation of the zinc enolate of thiopyridyl propionate gave only aldol products with no detectable  $\beta$ -lactone products, see: Abdel-Magid, A.; Pridgen, L. N.; Eggleston, D. S.; Lantos, I. *J. Am. Chem. Soc.* **1986**, *108*, 4595–4602.
- (29) A significant temperature dependence was observed for the ZnCl<sub>2</sub>-mediated TMAL process since no reaction occurred below 23 °C.
- (30) The diminished yield in this example is presumably due to facile decarboxylation to deliver the alkene and corresponds to the yield observed by Hirai (see ref 6).
- (31) (a) Suh, K.-H.; Choo, D.-J. *Tetrahedron Lett.* **1995**, *36*, 6109–6112. (b) Suh, K.-H.; Choo, D.-J. *Bull. Kor. Chem. Soc.* **1996**, *17*, 674–676.
- (32) (a) Bonamico, M.; Dessy, G.; Fares, V.; Scaramuzza, L. *J. Chem. Soc., Dalton Trans.* **1972**, *32*, 2515–2517. (b) Ashworth, C. C.; Bailey, N. A.; Johnson, M.; McCleverty, H. A.; Morrison, N.; Tabbiner, B. *J. Chem. Soc., Chem. Commun.* **1976**, 743–744. (c) Becker, B.; Radacki, K.; Wojnowski, W. *J. Organomet. Chem.* **1996**, *521*, 39–49. (d) Fraser, K. A.; Harding, M. M. *Acta Crystallogr.* **1967**, *22*, 75–80.
- (33) The TBS ketene acetal (*E*)-**2a** was utilized in NMR studies due to facile desilylation of the corresponding TES ketene acetal (*E*)-**2b**, which complicated spectral interpretation.
- (34) While it is well known that sp<sup>3</sup> silyl ether oxygens are significantly less Lewis basic than the corresponding sp<sup>3</sup> alkyl ether oxygens, far less information is available for sp<sup>2</sup> silyl ether oxygen atoms. Regarding the former, see: (a) Shambayati, S.; Blake, J. F.; Wierschke, S. G.; Jorgensen, W. L.; Schreiber, S. L. *J. Am. Chem. Soc.*

1990, 112, 697–703. (b) Keck, G. E.; Castellino, S. *Tetrahedron Lett.* 1987, 28, 281–284. (c) Keck, G. E.; Boden, E. P. *Tetrahedron Lett.* 1984, 25, 265–268.

(35) (a) Stanton, G. R.; Johnson, C. N.; Walsh, P. J. *J. Am. Chem. Soc.* 2010, 132, 4399–4408. (b) Stanton, G. R.; Koz, G.; Walsh, P. J. *J. Am. Chem. Soc.* 2011, 133, 7969–7976.

(36) Although we have found no published data for the solubility of  $\text{ZnCl}_2$  in  $\text{CH}_2\text{Cl}_2$ , we estimate, on the basis of our experiments, that it has a solubility of  $<0.002$  M.

(37) The downfield shift of the pyridine ring is not likely caused by a change in solvent polarity due to the low solubility of  $\text{ZnCl}_2$  in  $\text{CHCl}_3$ .

(38) Tan, T. S.; Mather, A. N.; Procter, G.; Davidson, A. H. *J. Chem. Soc., Chem. Commun.* 1984, 585–586.

(39) Ikeda, Y.; Ukai, J.; Ikeda, N.; Yamamoto, H. *Tetrahedron Lett.* 1984, 25, 5177–5180.

(40) The yield of the volatile lactol **15** was not determined because most of it was lost upon aqueous workup and silica gel purification. For related reactions, see: Denmark, S. E.; Henke, B. R.; Weber, E. *J. Am. Chem. Soc.* 1987, 109, 2512–2514 and references cited therein.

(41) The stereochemical assignment follows from analysis of  $^1\text{H}$  chemical shifts and comparison to those reported in the literature for the  $\alpha$ -methyl groups of *syn* ( $\delta$  1.1) and *anti* ( $\delta$  1.2) diastereomeric tetrahydrofuran methyl esters, see: (a) Mead, K. T.; Yang, H.-L. *Tetrahedron Lett.* 1989, 30, 6829–6832. (b) Gouzoulules, F. H.; Whitney, R. A. *Tetrahedron Lett.* 1980, 26, 3441–3445. (c) Bartlett, P. A.; Meadows, J. D.; Ottow, E. *J. Am. Chem. Soc.* 1984, 106, 5304–5311.

(42) The energies of E Conf2 and Z Conf1 are provided in the Supporting Information.

(43) Transition states are numbered on the basis of structural numbers for the starting material and product for each step; e.g., 22-23 refers to the transition state for conversion of **22** to **23**.

(44) The intermediate (*E*)-**22** is higher in energy than the Zn–O bond-breaking transition state, (*E*)-**22-23**, on the enthalpic surface because they are very close in energy and this transition state has a smaller zero-point energy than (*E*)-**22**. On the *E*(0 K) potential energy surface, the Zn–O bond-breaking transition state is 0.09 kcal/mol higher in energy than (*E*)-**22**.

(45) (a) Wilcox, C. S.; Babston, R. E. *J. Org. Chem.* 1984, 49, 1451–1453. (b) Babston, R. E.; Lynch, V.; Wilcox, C. S. *Tetrahedron Lett.* 1989, 30, 447–450. (c) For rationalization of diastereoselectivity in Mukaiyama aldol reactions based on conformational analysis of thioketene acetals, see: Annunziata, R.; Molteni, V.; Raimondi, L. *Magn. Reson. Chem.* 1996, 34, 858–864.

(46) (a) Lipscomb, W. N.; Strater, N. *Chem. Rev.* 1996, 96, 2375–2433. (b) Maret, W.; Li, Y. *Chem. Rev.* 2009, 109, 4682–4707.

(47) For a discussion of pseudorotation and dissociation/re-coordination pathways in the TMAL, see ref 20.

(48) Gung, B. W.; Wolf, M. A. *J. Org. Chem.* 1992, 57, 1370–1375.

(49) Kerr, J. A. In *CRC Handbook of Chemistry and Physics*, Lide, D. R., Ed.; CRC Press: New York, 1998–1999, pp 9-51–9-62.

(50) Carreira, E. M.; Singer, R. A. *Tetrahedron Lett.* 1994, 35, 4323–4326.